

# Development and topographic organization of subicular projections to lateral septum in the rat brain

Konstantinos I. Tsamis | Maria J. Lagartos Donato | Annelene G. Dahl | Kally C. O'Reilly | Menno P. Witter 

Kavli Institute for Systems Neuroscience, Centre for Computational Neuroscience, Egil and Pauline Braathen and Fred Kavli Centre for Cortical Microcircuits, NTNU Norwegian University of Science and Technology, Trondheim, Norway

## Correspondence

Menno P. Witter, Kavli Institute for Systems Neuroscience, Faculty of Medicine and Health Sciences, NTNU. Postbox 8905, NO-7491 Trondheim, Norway.  
Email: menno.witter@ntnu.no

## Present addresses

Konstantinos I. Tsamis, Neurosurgical Institute, Medical School, University of Ioannina, Ioannina, Greece

Maria J. Lagartos Donato, Department of Clinical Molecular Biology, University of Oslo and Akershus University Hospital, Lørenskog, Norway

Kally C. O'Reilly, Department of Psychiatry, Columbia University, New York State Psychiatric Institute, New York, New York

## Funding information

ENS, Grant/Award Number: 2014; Norges Forskningsråd, Grant/Award Number: 197467 and 223262; IBRO-PERC, Grant/Award Number: 2014; Genesis Pharma.

## Abstract

One of the main subcortical targets of hippocampal formation efferents is the lateral septum. Previous studies on the subicular projections, as a main output structure of the hippocampus, have shown a clear topographic organization of septal innervation, related to the origin of the fibres along the dorsoventral axis of the subiculum in the adult brain. In contrast, studies on the developing brain depict an extensive rearrangement of subicular projections during the prenatal period, shifting from the medial septum to the lateral septum. Our study aimed to describe the postnatal development of subicular projections to the septum. We injected anterograde tracers into the subiculum of 57 pups of different postnatal ages. Injections covered the proximodistal and dorsoventral axis of the subiculum. The age of the pups at day of tracer injection ranged from the day of birth to postnatal day 30. Analyses revealed that from the first postnatal day projections from subiculum preferentially target the lateral septum. Sparse innervation in the lateral septum was already present in the first few postnatal days, and during the following 3 weeks, the axonal distribution gradually expanded. Subicular projections to the lateral septum are topographically organized depending on the origin along the dorsoventral axis of the subiculum, in line with the adult innervation pattern. Different origins along the proximodistal axis of the subiculum are reflected in changes in the strength of septal innervation. The findings demonstrate that in case of the development of subicular projections, axonal expansion is more prominent than axonal pruning.

## KEY WORDS

axonal development, hippocampus, neural circuits, postnatal development, tracing

**Abbreviations:** AC, nucleus accumbens; BAC, bed nucleus of the anterior commissure; BDA, biotinylated dextran amine; BST, bed nucleus of the stria terminalis; cc, corpus callosum; dF, dorsal fimbria; F, fornix; Fi, fimbria; LS, lateral septum; MS, medial septal nucleus; PB, phosphate buffer; PFA, paraformaldehyde; SFi, septo-fimbrial nucleus; SHi, septo-hippocampal nucleus; SHy, septo-hypothalamic nucleus; SM, stria medullaris; SUB, subiculum; TS, triangular nucleus.

Edited by John Foxe.

The peer review history for this article is available at <https://publons.com/publon/10.1111/ejn.14696>.

This is an open access article under the terms of the Creative Commons Attribution-NonCommercial License, which permits use, distribution and reproduction in any medium, provided the original work is properly cited and is not used for commercial purposes.

© 2020 The Authors. *European Journal of Neuroscience* published by Federation of European Neuroscience Societies and John Wiley & Sons Ltd.

## 1 | INTRODUCTION

A close anatomical relation between the septum and the hippocampal formation is established via reciprocal connections. Studies in the mature brain of experimental non-primates revealed that all hippocampal subregions as well as parahippocampal regions receive septal innervation originating from the medial septum and diagonal band of Broca (Amaral & Kurz, 1985; Baisden, Woodruff, & Hoover, 1984; Gaykema et al., 1990; Meibach & Siegel, 1977b; Unal, Joshi, Viney, Kis, & Somogyi, 2015). The septum is also the main subcortical target of hippocampal efferent projections. The latter projections originate in the hippocampal areas CA1, CA3 and subiculum, and terminate mainly in the lateral septum (LS), although sparse innervation of the medial septum and diagonal band of Broca has also been observed (Gaykema, Kuil, Hersh, & Luiten, 1991; Meibach & Siegel, 1977a; Nyakas, Luiten, Spencer, & Traber, 1987; Swanson & Cowan, 1977, 1979; Witter & Groenewegen, 1986).

The subiculum, as a major output structure of the hippocampus, projects by way of the fornix to LS. In the adult rodent, these projections are topographically organized, depending on the origin along the longitudinal axis of the hippocampal formation. Dorsal parts of the subiculum innervate dorsomedial parts of LS, and ventral parts of subiculum innervate ventrolateral parts of LS (Meibach & Siegel, 1977a). An additional organizational feature is that subicular projections to LS mainly originate from the proximal part of the subiculum (Witter, Ostendorf, & Groenewegen, 1990).

Behavioural and physiological studies have highlighted the relevance of septo-hippocampal connections for encoding, consolidation and retrieval processes in the hippocampus and thus implicated them in learning and memory, in both spatial and non-spatial settings (Easton, Douchamps, Eacott, & Lever, 2012; Hunsaker, Rogers, & Kesner, 2007; Okada & Okaichi, 2010; Parent & Baxter, 2004). Connections between the medial septum and hippocampus have been extensively studied, as have their role in hippocampal oscillatory activity, in particular in the theta frequency (Tsanov, 2015). Disruption of the inputs from the medial septum strongly affects theta rhythmicity in the hippocampus and can provoke the occurrence of abnormal excitability states, such as epilepsy (Colom, 2006; Kitchigina et al., 2013). On the other hand, the efferent connections from the hippocampus to LS are involved in the processing and integration of spatial information in the environment (Zhou, Tamura, Kuriwaki, & Ono, 1999), in the regulation of speed of locomotion (Bender et al., 2015), as well as in reward, addiction and emotional processing (Calfa, Bussolino, & Molina, 2007; Hunsaker, Tran, & Kesner, 2009; Jonsson, Morud, Stomberg, Ericson, & Soderpalm, 2017; McGlinchey & Aston-Jones, 2017; Zoicas, Slattery, & Neumann, 2014).

Not much is known about the development of the septo-hippocampal connections. An early study, based on terminal degeneration after hippocampal lesions in the rat brain, reported evidence for the presence of hippocampal efferent projections to the septum already at birth (Singh, 1977). Another study in the mouse reported that hippocampo-septal fibres start developing from the early embryonic life (at E15), before the first reciprocal septal fibres can be detected in the hippocampus (at E17) (Super & Soriano, 1994). The early hippocampo-septal projections terminate in the medial septum, and during perinatal development, they reshape, such that they eventually target LS (Linke, Pabst, & Frotscher, 1995).

In the present study, we add to this sparse developmental data by analysing the postnatal development of subicular projections to LS in the rat brain. The aim of the study was to examine when in the postnatal period the topographic organization of the subicular fibres in LS, as seen in adults, becomes established. Our data corroborate the available sparse data on the development of subicular projections to LS and the dorsoventral axis of organization, and we add more details to the relevance of the origin along the proximodistal, or transverse, axis. Our data further indicate that these topographical axes of organization are already visible in young postnatal stages and that changes during development are mainly observed in the density and overall levels of branching of terminal subicular axons in LS. The latter observation that increased axonal branching is more apparent that axonal pruning is similar to what has been reported for the development of other connections in the hippocampal system (Haugland, Sugar, & Witter, 2019; O'Reilly, Gulden Dahl, Ulsaker Kruge, & Witter, 2013; Sugar, Witter, Strien, & Cappaert, 2011).

## 2 | MATERIALS AND METHODS

### 2.1 | Animal information and breeding

We used 57 Long Evans pups in the study. Breeding groups, consisting of up to three females and one male, were housed in enriched cages containing toys, with free access to food and water and 12:12-hr reversed light/dark cycle. Cages were checked twice daily, in the morning and the evening for pups, and the day pups were observed was considered postnatal day 0 (P0). The litter size was culled to ten pups by P3. Pups were allowed to remain in the nest with the mother until weaning at P21. All procedures were approved by the Norwegian Food Safety Authority as well as the Local Animal Welfare Committee of the Norwegian University of Science and Technology, and adhered to the rules and directives set by the Norwegian Animal Welfare Act and the European Community on animal well-being (European directive 2010/63 on the protection of animals

used for scientific purposes). Both male and female pups were used for the study.

## 2.2 | Surgery procedure

Surgeries were conducted under isoflurane anaesthesia, using a neonatal mask for the period P0–13 (Kopf, Model 973-B). The width of the palate bar of the neonatal mask was adjusted to make it fit inside the mouth of these young pups. We used a small adult mask (Kopf, Model 906) in case of older animals (P14–adult). Animals were head-fixed with zygoma ear cups (Kopf, Model 921). Before incision, the skin was disinfected with 2% iodine in the 65% ethanol, and a local analgesic (0.2 ml per 100g body weight of a 0.5 mg/ml solution; Marcain, Astra Zeneca) was injected subcutaneously at the place of the incision.

Up to 50  $\mu$ l/g body weight of saline was administered subcutaneously throughout the course of the surgery to avoid dehydration. Animals were also administered carprofen as a postsurgery analgesic (1 ml per 100 g body weight of a 0.5 mg/ml solution; Rimadyl, Pfizer).

For the injections, a hole was drilled in the skull. The anterograde tracers biotinylated dextran amine (BDA, 5% in phosphate buffer (PB; 0.125M in H<sub>2</sub>O; PH 7.4), 10,000 MW, cat# 1956; Invitrogen, Eugene, OR) or Alexa 488-conjugated dextran amine (5% in PB; Alexa 488 DA, cat# D22910, Invitrogen) were iontophoretically injected through a glass micropipette of 20–25  $\mu$ m outer diameter (30–0044; Harvard Apparatus; pulled with a PP-830 Puller, Narishige) into the subiculum (5–6  $\mu$ A alternating positive currents, 6-s on/6-s off, for 5–12 min; 51,595; Stoelting Europe). After surgery, rat pups were allowed to recover to an awake state under a heating lamp. When fully awake, rat pups were returned to maternal care until time of kill, which was selected to be as short as possible. Following established procedures, for P0–13 rat pups the survival time was set at 24 hr after injection and a range between 24 and 48 hr for P14–30 rat pups, depending on the initial body weight of the pup. In this way, we secured sufficient visualization of the connectivity and obtained an as precise as possible age estimate during the development (O'Reilly et al., 2013). A total of 57 injections were successfully placed along the proximodistal axis of the dorsal, intermediate and ventral subiculum of the pups with ages ranging between P1 and P30 at day of tracer injection (see table 1).

## 2.3 | Brain tissue collection, histology and immunohistochemistry

All animals were transcardially perfused under terminal isoflurane anaesthesia. Animals were perfused with saline through the left ventricle until the flow out of the right atrium was clear, followed by 4% paraformaldehyde (PFA; Merck,

#140, Darmstadt) until the body was sufficiently stiff. The brains were extracted and left in PFA for 24–48 hr before being moved to a cryoprotective solution (20% glycerol, 2% dimethylsulphoxide in 125 mM phosphate buffer or PB, pH 7.4). Fifty-micrometre horizontal sections were cut with the use of a freezing microtome (Thermo Scientific). Sections were collected in six equally spaced series, and the first series was mounted on superfrost plus slides (Menzel-Gläser [Gerhard Menzel GmbH]/art. nr. J1800AMNZ) and dried overnight on a warming plate at 30°C for subsequent Nissl staining with cresyl violet. The other series were placed in the cryoprotecting solution and stored at –20°C.

To visualize BDA, free-floating sections were washed in 125 mM PB three times for 10 min each. Endogenous peroxidases were blocked in three washes with 3% hydrogen peroxide in PB for 10 min each, and then washed again in PB three times for 10 min each. The sections were subsequently washed in TBS-TX (50 mM Tris, 150 mM NaCl, 0.5% Triton X, pH 8.0) three times for 10 min each, followed by a 90-min incubation with avidin–biotin–peroxidase in TBS-TX (VECTASTAIN ABC Kit; Vector Labs) according to manufacturer's instructions or with Alexa-conjugated streptavidin (Alexa 546, S11225, Invitrogen). In the cases where avidin–biotin–peroxidase was used, the sections were then incubated for 15 min in a DAB-peroxidase solution containing 5 mg diaminobenzidine (DAB; Sigma-Aldrich Co., LLC./art. nr. B5905) and 3.3 ml H<sub>2</sub>O<sub>2</sub> in 10 ml Tris-HCl. Irrespective of whether the incubations were carried out with Alexa-conjugated streptavidin or DAB, the sections were rinsed three times for 5 min in Tris-HCl and mounted on glass slides, dried overnight, cleared in toluene, coverslipped with entellan (Merck Darmstadt, cat# 107,961) and viewed with brightfield or darkfield microscopy. In some cases, Nissl staining was necessary to aid the delineation of brain regions. Delineations of the hippocampal formation followed published nomenclatures in adult and postnatal rats (Cappaert, Strien, & Witter, 2015; O'Reilly et al., 2013), and for delineations of LS, we refer to the work of Risold and Swanson (1997).

## 2.4 | Image analysis

The image acquisition and comparison of anterograde labelling was performed using a slide scanner, equipped for either brightfield or fluorescent imaging (Zeiss Mirax Midi 20X NA 0.8). The images were then adjusted in Adobe Photoshop CS6 (version 13.0.0) to assure equal quality of image reproduction. To compare the injection sites, relevant injections were mapped onto a standard series of sections taken from one P15 animal. To create a map of the overlays for illustrative purposes, three separate images were false-coloured in three different colours and overlaid on top of one another.

**TABLE 1** Information of animals used in the study

Information of the animals used in the study					
	Number	Age	Sex	Tracer	Injection site
1	17,074	P14	F	BDA	SUB intermediate
2	16,972	P15	M	BDA	SUB intermediate/CA1
3	17,058	P14	M	BDA	SUB intermediate
4	17,073	P14	F	BDA	SUB intermediate/MEC
5	17,052	P7	F	BDA	SUB intermediate/CA1
6	17,041	P7	M	BDA	SUB intermediate
7	16,617	P14	F	BDA	SUB intermediate
8	17,053	P7	M	BDA	SUB intermediate
9	16,616	P14	M	BDA	SUB intermediate
10	17,075	P14	F	BDA	SUB intermediate/MEC
11	17,057	P14	M	BDA	SUB intermediate
12	17,038	P14	F	BDA	SUB intermediate
13	16,975	P14	M	BDA	SUB intermediate
14	15,598	P15	F	BDA	SUB intermediate
15	17,072	P7	M	BDA	SUB intermediate
16	17,054	P7	M	BDA	SUB intermediate
17	17,040	P7	M	BDA	SUB intermediate/PrS
18	17,037	P14	F	BDA	SUB intermediate
19	17,036	P13	F	BDA	SUB intermediate
20	16,514	P14	F	BDA	SUB intermediate/PrS
21	15,884	P17	F	BDA	SUB intermediate
22	15,881	P15	F	BDA	SUB intermediate
23	16,940	P27	M	BDA	SUB dorsal/DG
24	16,939	P27	F	BDA	SUB dorsal
25	16,197	P30	M	BDA	SUB dorsal/PrS
26	16,185	P23	M	BDA	SUB dorsal/PrS
27	15,883	P15	F	BDA	SUB dorsal/DG
28	15,351	P10	F	BDA	SUB dorsal/CA1
29	15,336	P4	F	BDA	SUB dorsal
30	15,071	P2	M	BDA	SUB dorsal
31	13,590	P16	F	BDA	SUB dorsal/CA1
32	13,587	P14	F	BDA	SUB dorsal/CA1
33	14,255	P11	F	BDA	SUB dorsal
34	14,269	P7	F	BDA	SUB dorsal
35	14,295	P2	M	BDA	SUB dorsal/CA1
36	13,580	P11	F	BDA	SUB dorsal
37	16,186	P23	F	BDA	SUB ventral/PrS
38	15,197	P6	M	BDA	SUB ventral/CA1
39	15,189	P1	M	BDA	SUB ventral/CA1
40	20,999	P9	M	BDA	SUB ventral/CA1
41	21,000	P15	F	BDA/DA488	SUB ventral
42	21,309	P12	F	BDA	SUB ventral
43	21,321	P11	F	BDA	SUB ventral/CA1

(Continues)

TABLE 1 (Continued)

Information of the animals used in the study					
44	21,374	P11	F	BDA	SUB ventral
45	21,375	P15	F	BDA/DA488	SUB ventral
46	20,909	P21	M	BDA/DA488	SUB ventral
47	21,032	P6	M	BDA	SUB ventral
48	21,200	P17	F	BDA/DA488	SUB ventral
49	21,529	P9	M	BDA/DA488	SUB ventral
50	21,532	P16	F	BDA	SUB ventral
51	21,717	P18	F	BDA/DA488	SUB ventral/DG
52	21,535	P20	M	BDA/DA488	SUB ventral
53	21,996	P20	M	BDA/DA488	SUB ventral
54	19,952	P3	F	BDA	SUB ventral/PrS
55	22,058	P24	M	BDA/DA488	SUB ventral
56	22,785	P3	F	BDA	SUB ventral
57	22,239	P3	M	BDA	SUB ventral/PrS

Note: We provide the animal experimental number, postnatal age of tracer injection in days, gender, anterograde tracer used: biotinylated dextran amine (BDA and/or dextran amine 466 (DA466) and location of injection site for all 57 animals analysed for this study. Abbreviations: DG, dentate gyrus; F, female; M, male; MEC, medial entorhinal cortex; PrS, presubiculum; SUB, subiculum.

As injection sites and terminal distribution are not always in the same section, these overlays were made by mapping both onto the horizontal section that showed the clearest terminal labelling. Local hippocampal landmarks were used to determine the scaling of individual images. At all ages, the cytoarchitectonic features were used for the identification of all hippocampal/parahippocampal subfields and septal areas. Part of the material used in this study was previously used to describe the development of the projections from the subiculum area to the parahippocampal area (O'Reilly et al., 2013). By reusing already acquired data to analyse a new target of subicular projections, we are minimizing the number of animals used in experiments.

### 3 | RESULTS

The subiculum is a part of the hippocampal formation and is wedged in between the hippocampus proper (CA fields) and the parahippocampal region. It follows the overall 3-dimensional shape of the hippocampus, and its organization is thus generally described using two main topographical axes, the longitudinal or dorsoventral axis and the transverse or proximodistal axis. The dorsoventral axis starts dorsally at the mediodorsal tip, which is closely associated with the septal complex, to the lateroventral tip, which is associated with the amygdaloid complex. The proximodistal axis is oriented perpendicular to the dorsoventral axis, where proximal indicates the part of the subiculum closest to CA1, and distal indicates the part closest to the parahippocampal area referred to as presubiculum (Cappaert et al., 2015).

A total of 57 injections in subiculum were used in the present study. The age of the pups at day of tracer injection in subiculum ranged from P1 to P30 (Table 1). In view of the age distribution in our data set and our aim to address when an adult topographical organization is apparent, we organized the results as to first address the presence of a topographical organization along the proximodistal subicular axis, for which we have the densest data set at the end of second postnatal week, and compared those with data at the end of the first postnatal week. These data are derived from injections at an intermediate dorsoventral level of the subiculum. We subsequently compare these data with a data set spanning the same developmental window but including dorsal and ventral levels of the subiculum. Finally, we describe data obtained in very young animals (P0-5) and add observations in animals older than P15, both covering the proximodistal as well as the dorsoventral organization.

#### 3.1 | Proximodistal organization of subicular projections to lateral septum at the end of the second postnatal week

Animals at the end of the second postnatal week ( $n = 14$ , P13-P15) were used in order to analyse the topographic organization in the septum of fibres originating from different areas along the transverse (proximodistal) axis of subiculum, at an intermediate dorsoventral level. Part of this material was previously used to describe the development of the projections from subiculum area to the parahippocampal area, and the exact mapping of the injections along the transverse axis of subiculum can be found there (O'Reilly et al., 2013). For descriptive reasons, injections

are grouped into three groups: proximal ( $n = 4$ ), intermediate ( $n = 6$ ) and distal ( $n = 4$ ) injections.

### 3.1.1 | Proximal subicular projections

After tracer injection in the proximal subiculum at an intermediate dorsoventral level, all four cases resulted in a similar pattern of septal labelling as illustrated for a representative case (Figure 1). Fibres could be followed in the fimbria, reaching the dorsal, caudo-lateral tip of the septum. At this level, they did not enter LS but continued in the fimbria in a ventromedial direction (Figure 1a). Throughout this course, subicular fibres were rarely seen to have varicosities, indicating an overall absence of en passant synapses, and did not give off many terminating collaterals. Labelled fibres were mostly restricted to the area occupied by the fimbria and the septo-fimbrial nucleus, and they occasionally entered the triangular septal nucleus. Labelled fibres started entering LS at an intermediate medio-lateral and dorsoventral level of LS (Figure 1b). At this point of entry, fibres were seen to bifurcate, whereas others just curved, changing direction and entering LS. Within LS, the fibres continued ventrally and rostro-laterally, giving off collaterals as well as showing varicosities with an increasing density (Figure 1c). At more ventral levels, labelling became weaker with the terminal field occupying the rostral parts of LS, with some fibres continuing towards the nucleus accumbens (Figure 1d-f). On their course through LS, the labelled fibres were mainly located in the cytoarchitecturally defined intermediate lateral septal nucleus. However, few fibres entered the medial septal nucleus at its dorsal part (Figure 1e) and showed varicosities or some sparse terminating collaterals. Few fibres entered the ventral part of the dorsal lateral septal nucleus and the dorsal part of the ventral lateral septal nucleus. Upon leaving LS, many labelled fibres continued their course towards the midline, where they curved posterovertrally to enter the postcommissural fornix, at the same time contributing to very scarce innervation of the posterior and ventral group of septal nuclei (Figure 1d-f).

### 3.1.2 | Intermediate proximodistal subicular projections

Injections at an intermediate proximodistal position but at the same intermediate dorsoventral level as the previous and subsequent cases resulted in a similar pattern of septum innervation with that described for proximal injections, for all six animals examined (Figure 2). Fibres from the fimbria (Figure 2a, b) started entering LS at an intermediate medio-lateral and dorsoventral level (Figure 2c), heading in a ventral and rostro-caudal direction. Both terminating fibres and passing fibres with and without varicosities were observed (Figure

2d-f). However, the total amount of fibres that entered LS after intermediate subicular injections was reduced compared with proximal injections. Terminating fibres or passing fibres with varicosities were sparsely observed in the septo-fimbrial, triangular, medial septal, dorsal and ventral lateral nuclei (Figure 2e-f), as previously described for the proximal injections.

### 3.1.3 | Distal subicular projections

Fibres labelled after tracer injections at the distal part of subiculum could also be followed reaching the septal area through the fimbria (Figure 3). At an intermediate medio-lateral and dorsoventral level of LS, as previously described for proximal and intermediate injections, some fibres entered LS (Figure 3b-d). However, the overall density of labelling was much weaker than seen after proximal and intermediate injections. The innervation pattern of the other septal nuclei was also very sparse. In contrast, many fibres continued their course in the postcommissural fornix, leaving the septum (Figure 3d-f). Although differences in the size of the injection sites will influence the amount of labelling, it is clear from the data that the proportion of fimbria fibres that continue in the fornix, travelling past or through the septum, gradually increased from proximal to distal subicular injections. Part of these fibres continued to the stria medullaris (Figure 3e) and reached the anterior thalamic nuclei as well as sending terminating collaterals around the stria medullaris, and into the dorsal tip of the bed nucleus of stria medullaris.

The dorsoventral level at which fibres from the fimbria enter LS was found to be the same for all intermediate subicular injections and restricted to a depth of 750 to 2,000  $\mu\text{m}$  ventrally from the dorsal tip of the septum, with the vast majority of the fibres entering around the depth of 1,250  $\mu\text{m}$ . This was consistent for all injections along the proximodistal axis of the subiculum at an intermediate dorsoventral level. However, the density of labelled fibres terminating in LS was gradually reduced related to the position of the injections from proximal, through intermediate, to distal subiculum.

## 3.2 | Projections to the septum from the border area between CA1 and subiculum

### 3.2.1 | CA1-subiculum border projections

In one animal, the injection involved the border between CA1 and subiculum at approximately the same intermediate dorsoventral level as the previously described cases, involving neurons of both areas (Figure 4). Like in the previous cases, fibres could be followed in the fimbria reaching the dorsal, caudo-lateral tip of the septum. Already at this level,

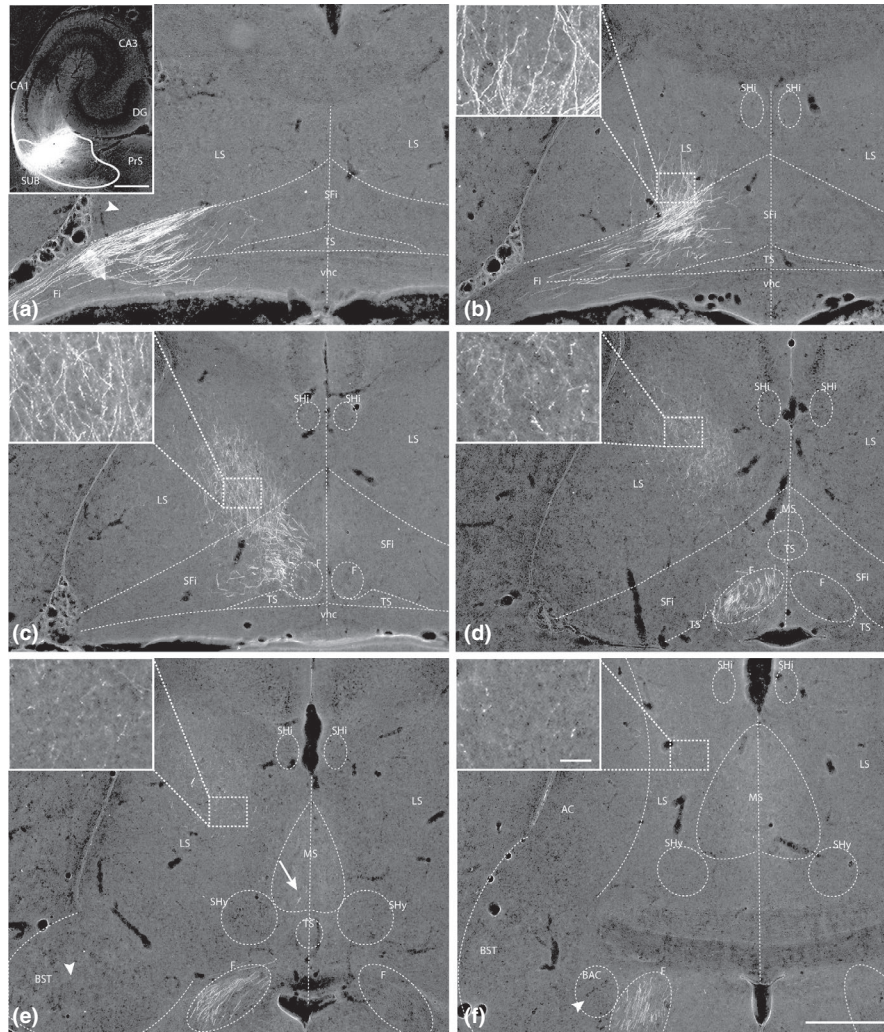


**FIGURE 1** Labelling in the septum resulting from an injection into proximal subiculum of a P15 rat. Inset in a: injection site. Scale bar: 500  $\mu\text{m}$ . (a–f), Horizontal sections through the septum with 600  $\mu\text{m}$  dorsoventral spacing between each two levels depicted from dorsal (a) to ventral (f). (a), Labelled fibres in the fimbria (Fi) reaching the dorsal septum. Fibres do not enter LS (arrowhead) but continue in the fimbria and septo-fimbrial nucleus (SFi) heading into a ventromedial direction. (b), Horizontal section taken at the point of entry of fibres into LS (inset represents a higher magnification of the boxed area in this and all subsequent figures). (c), Next level section illustrating a densely labelled plexus in LS of passing fibres with and without varicosities as well as terminating collaterals. The fibres mainly travel ventrally and rostro-laterally. (d), Horizontal section taken at the dorsal tip of medial septal nucleus (MS). At this level, more terminating fibres occupy LS. Many fibres continue in the fornix (F). (e), A more ventral level shows the terminal field in the rostral part of LS. At this level, few labelled fibres are present in MS (arrow), and no fibres are apparent in the bed nucleus of the stria terminalis (BST) (arrowhead). (f), The terminal field in the most ventral part of LS is sparse. Some labelled fibres are present in the nucleus accumbens (AC), whereas no fibres can be seen into the bed nucleus of the anterior commissure (BAC) (arrowhead) or BST. Scale bar in f equals 500  $\mu\text{m}$  (valid for a–f). Scale bar in the higher magnification image in f equals 50  $\mu\text{m}$  (valid for the magnification squares in b–f)

the fibres started to enter into LS and branched into terminating collaterals, occupying the whole rostro-caudal extent of LS, extending in a strip-like form from the dorsolateral side to a ventromedial position (Figure 4a–b). However, it is again at an intermediate medio-lateral and dorsoventral level of LS that we saw a massive change in the course of the fibres, so that many fibres curved, leaving the fimbria and entering LS. This level is identical to where the previously described subicular fibres entered LS (Figure 4c–d). Fibres that already entered LS expanded their terminating field in

a rostro-ventral direction occupying the anterior part of LS and continued to the adjacent nucleus accumbens (Figure 4e–f). Ventrally from that level, many fibres continued their course in the postcommissural fornix, again like what we described above for subicular injections. Noteworthy observations related to this injection site were some isolated fibres that could be seen in the contralateral LS (Figure 4e) and the relatively strong innervation observed in bed nucleus of the anterior commissure and bed nucleus of the stria terminalis (Figure 4f).

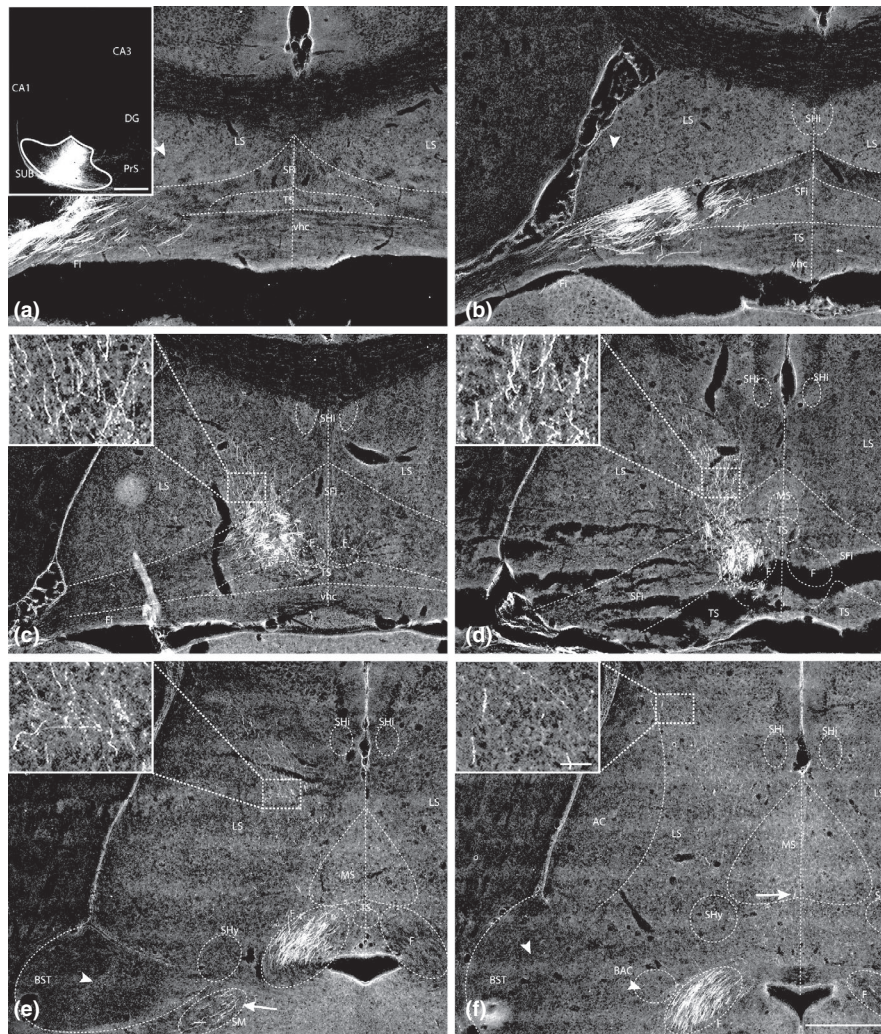


**FIGURE 2** Labelling in the septum following an injection into mid-transverse subiculum of a P15 rat. Inset in a: injection site. Scale bar: 500  $\mu\text{m}$ . (a–f), Horizontal sections through septum with 600  $\mu\text{m}$  dorsoventral spacing between each two levels depicted from dorsal (a) to ventral (f). (a–b), Labelled fibres in the fimbria (Fi) reaching the septum at dorsal levels. The fibres do not seem to enter LS (arrowheads) at this level, but they continue in the fimbria and septo-fimbrial nucleus (SFi) towards a ventromedial direction. (c–d), Horizontal sections taken at intermediate dorsoventral level of the LS showing the entry point of labelled fibres in LS. Within LS, the labelled passing fibres with and without varicosities travel ventrally and rostro-laterally, giving off terminal collaterals (see high power insets). (e–f), Sections at ventral levels of LS. Terminating fibres occupy the rostral part of LS. Many fibres continue their course within the fornix although few continue as part of the stria medullaris (SM) (arrow in e). Few labelled fibres are present in MS (arrow in f). No fibres are seen in the bed nuclei of the stria terminalis (BST) and the anterior commissure (BAC) (arrowheads). Scale bar in f equals 500  $\mu\text{m}$  (valid for a–f). Scale bar in the higher magnification box in f equals 50  $\mu\text{m}$  (valid for the magnification squares in c–f)

### 3.3 | Topographical organization of subicular projections to lateral septum at the end of the first postnatal week

#### 3.3.1 | Proximodistal organization

Animals at the end of the first postnatal week ( $n = 5$ , P7) were used to analyse the early development and topographic organization in the septum of fibres originating from different areas along the transverse proximodistal axis of the subiculum, again taken at an intermediate dorsoventral level. Part

of this material was previously used to describe the development of the projections from subiculum area to the parahippocampal area, and the exact mapping of the injections along the transverse axis of subiculum can be found there (O'Reilly et al., 2013). The cases were grouped into three groups related to the injection site in subiculum: proximal ( $n = 1$ ), intermediate ( $n = 1$ ) and distal ( $n = 3$ ), as previously described for P13–P15 animals.

The innervation pattern of LS at this age (Figure 5) was identical to that observed at P13–P15 animals. Moreover, the gradual reduction in the amount of subicular projections

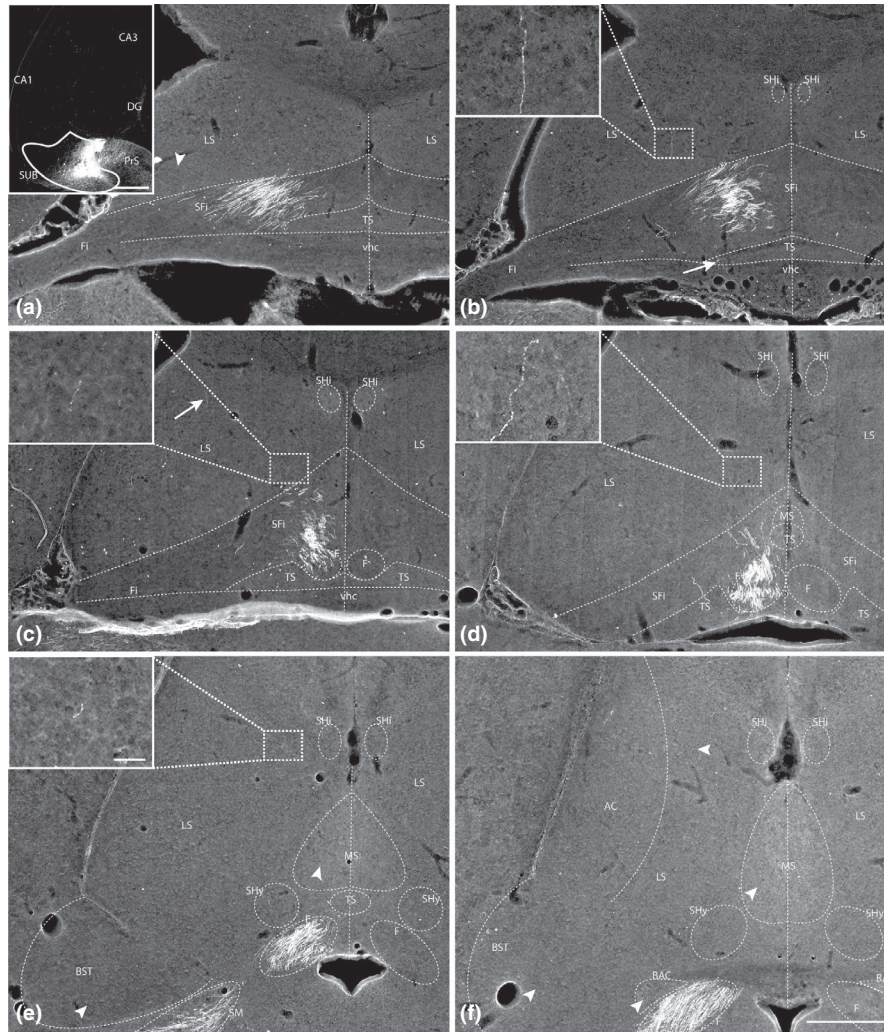


**FIGURE 3** Labelling in the septum following an injection into distal subiculum of a P15 rat. Inset in a: injection site. Scale bar: 500  $\mu\text{m}$ . (a–f), Horizontal sections through septum with 600  $\mu\text{m}$  dorsoventral spacing between each two levels depicted from dorsal (a) to ventral (f). (a), Labeled fibres in fimbria (Fi) reaching the septum at dorsal levels. The fibres do not seem to enter LS (arrowhead) at this level. (b–d), Horizontal sections taken at intermediate dorsoventral level of LS showing the entry point of fibres in LS. A few labeled fibres can be seen in LS (boxed area and arrow in c), although many fibres continue their course within the fornix (F) and few continue as part of the stria medullaris (SM). Arrow in b shows labeled fibres in the triangular septal nucleus (TS). (e–f), Sections at ventral levels of LS. Few terminating fibres can be seen at the rostral part of LS (magnification box). No labeled fibres can be seen in this case in the ventral part of the LS, neither in the medial septal nucleus (MS), nor in the bed nuclei of the stria terminalis (BST) and the anterior commissure (BAC) (arrowheads). Scale bar in f equals 500  $\mu\text{m}$  (valid for a–f). Scale bar in the higher magnification box in e equals 50  $\mu\text{m}$  (valid for the magnification squares in b–e). Note the striking difference in the amount of fibres innervating the LS after distal subicular injection compared with proximal and intermediate injections in Figures 1 and 2

to LS dependent on the origin along the proximodistal axis, as reported above, was also apparent in P7 animals. So, in order to avoid repetitions, we only refer here to the differences observed. The overall amount of fibres observed in the septum was estimated to be slightly reduced for P7 animals than in older animals with injections in corresponding subicular sites. Furthermore, the innervation of medial, posterior and ventral septal nuclei appeared even sparser in the P7 animals than in P13–P15 animals. Compared with older animals, fibres of P7 animals displayed sparser collaterals at terminating points but more varicosities throughout

their course, some of which were very large especially close to branching points and where fibres entered LS (Figure 5b, d).

One more P7 case was examined with an injection involving mainly the proximal subiculum with some involvement of distal CA1 neurons (border CA1–subiculum). In this case, some fibres entered LS upon reaching the dorsal, caudo-lateral tip of the septum but at an intermediate medio-lateral and dorsoventral level of LS more fibres entered LS, expressing an innervation pattern similar to that described for a P14 case with the injection addressed to the

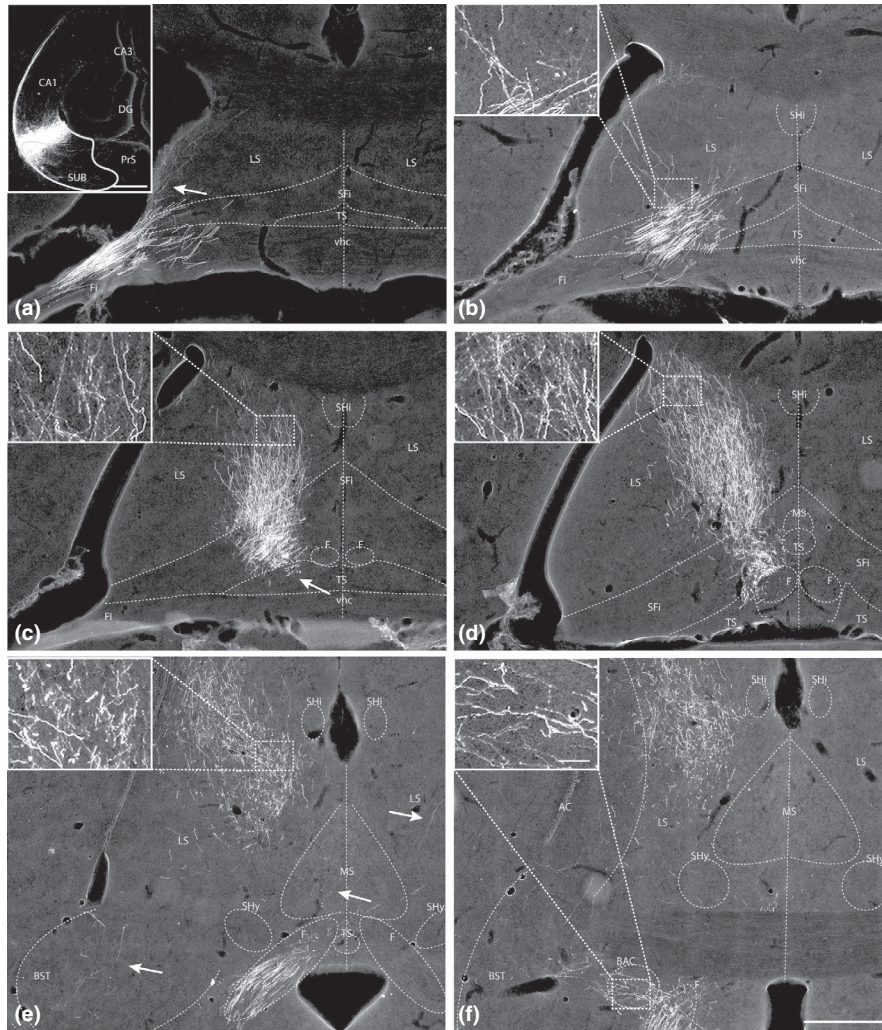


**FIGURE 4** Labelling in the septum following an injection applied to the border between CA1 and the subiculum of a P15 rat. Inset in a: injection site. Scale bar: 500  $\mu\text{m}$ . (a–f), Horizontal sections through the septum with 600  $\mu\text{m}$  dorsoventral spacing between each two levels depicted from dorsal (a) to ventral (f). (a–b), Labelled fibres in the fimbria (Fi) reaching the septum at dorsal levels. The fibres start entering in LS at this level and they branch into thin terminating collaterals, occupying the whole rostro-caudal extent of the LS and extending in a strip-like fashion from the dorsolateral side of the LS to a ventromedial direction. (c–d), At intermediate dorsoventral levels of the LS, many fibres from the Fi and the septo-fimbrial nucleus (SFf) curve and enter the LS. Within LS, the labelled fibres with and without varicosities travel ventrally and rostro-laterally, giving off terminal collaterals. (e–f), Sections at ventral levels of LS. Terminating fibres occupy the rostral part of LS (e, boxed area). Many fibres continue their course within the fornix (F). Besides, few labelled fibres can be seen in MS, as well as in contralateral LS (arrows). Significant innervation can also be seen in the bed nuclei of the stria terminalis (BST) (arrow) and the anterior commissure (BAC; boxed area). Scale bar in f equals 500  $\mu\text{m}$  (valid for a–f). Scale bar in the higher magnification box in f equals 50  $\mu\text{m}$  (valid for the magnification squares in b–f)

border between CA1 and subiculum (Figure 4). Innervation of the bed nucleus of the anterior commissure and the bed nucleus of the stria terminalis was also observed in this case.

The dorsoventral level at which fibres from the fimbria entered LS for P7 animals with intermediate subicular injections was restricted to a depth of 500 to 1,500  $\mu\text{m}$  ventrally from the dorsal tip of the septum, with the vast majority of the fibres entering around the depth of 1,000  $\mu\text{m}$ . This was consistent for all injections along the proximodistal axis of the subiculum at an intermediate dorsoventral level. This level is slightly less ventral than in case of the P13 animals,

likely reflecting the overall smaller size of the brain in the P7 animals.

### 3.4 | Dorsoventral organization of developing subicular projections to lateral septum

In order to assess the development and organization of projections to LS originating from different dorsoventral sites of subiculum, we also analysed injections of anterograde tracers into dorsal and ventral subiculum.

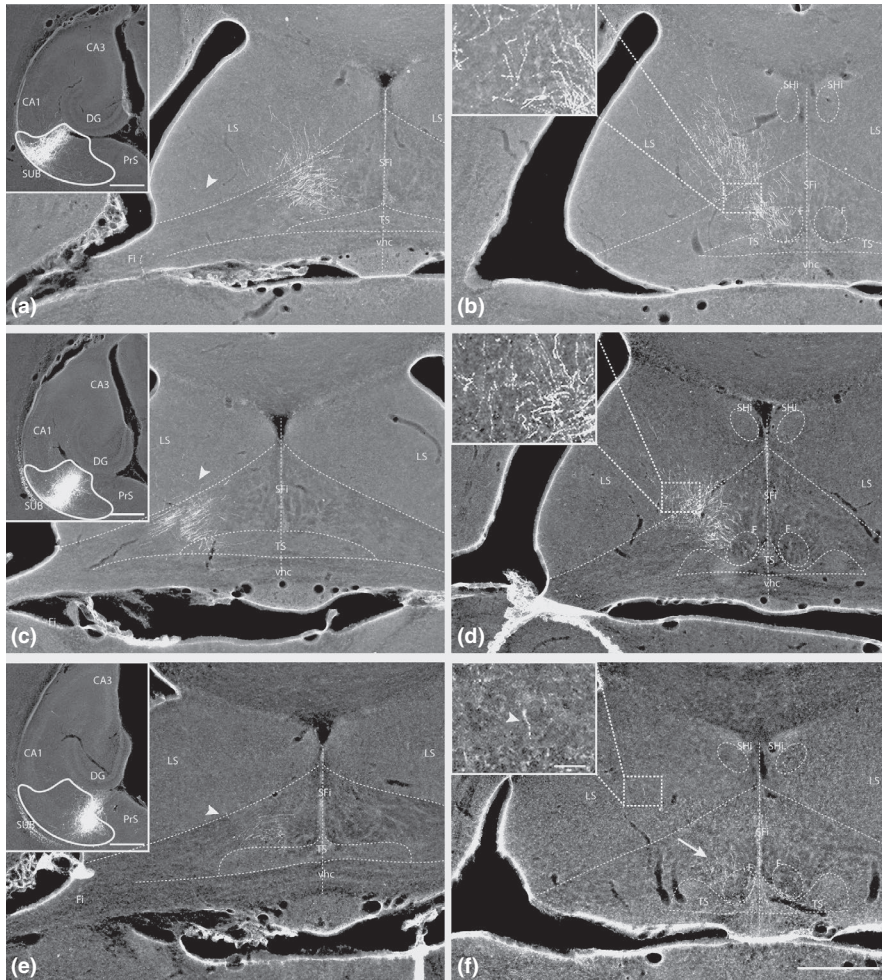


**FIGURE 5** Labelling in the septum resulting from three representative injections at approximately the same intermediate dorsoventral level into proximal (a, b), intermediate (c, d) and distal (e, f) parts of the subiculum in P7 old pups. Insets in a, c and e: injection sites. Scale bar: 500  $\mu\text{m}$ . (a, c, e), Horizontal sections taken at the level were labelled fibres in the fimbria (Fi) start entering LS (arrowheads). Note the difference in the density of these fibres from (a to c and e. b, d, f), Horizontal sections at intermediate dorsoventral level of the LS. There is a clear reduction in the innervation density of LS from b to f, such that in f only a couple of fibres can be observed in LS. Insets in b and f show fibres leaving SFi to enter LS expressing few collaterals and many varicosities throughout their course, some of which are very large especially close to branching points. Scale bar in f equals 500  $\mu\text{m}$  (valid for a–f). Scale bar in the higher magnification box in f equals 50  $\mu\text{m}$  (valid for the magnification boxes in b, d, f)

### 3.4.1 | Dorsal subicular projections

Among the injections successfully targeting the dorsal subiculum ( $n = 7$ , P7–P16), three involved the proximal subiculum and adjacent CA1 area, three were restricted to the subiculum, mainly centred along the proximodistal axis, and one involved the distal and intermediate subiculum as well as molecular layer of dentate gyrus.

Following the course of fibres in the three cases with injections restricted to the subiculum (Figure 6), fibres could be found to curve around the dorsal end of the hippocampus reaching the dorsal extremity of the septum (Figure 6b). At this level, they did not enter LS, but they continued in the fimbria in a ventromedial direction (Figure 6c). Throughout the course in the fimbria, subicular fibres were rarely seen to have large varicosities or terminating fibre collaterals. When present, terminal fibres were mostly restricted to the area involving the fimbria and septo-fimbrial nucleus, but they were also occasionally seen to enter the triangular septal nucleus. At increasingly more ventral levels, the labelled fibres reached the midline and fibres started entering LS, at a medial medio-lateral level and intermediate dorsoventral level of LS (Figure 6d), so very similar to the position described for

the projections originating in the intermediate dorsoventral levels (see above). At the point of entry, some fibres bifurcated and some just curved, changing direction and entering LS. In LS, passing fibres with and without varicosities as well as terminating collaterals took an overall rostro-ventral orientation. At more ventral levels, the position of the terminating fibres shifted towards a more lateral and rostral position, eventually occupying the rostral parts of LS, with some fibres continuing towards the nucleus accumbens (Figure 6e–f). At their course throughout LS, fibres were mainly located in the intermediate lateral septal nucleus. The fibres seemed to avoid passing by the area occupied by the septo-hippocampal nucleus, but terminating collaterals were often observed in the latter nucleus (Figure 6d–f). Furthermore, few fibres entered the medial septal nucleus dorsally and expressed varicosities and a few terminating collaterals. No fibres were found in ventral and dorsal lateral septal nuclei. After leaving the LS, the labelled fibres curved posteroventrally to join the fornix (Figure 6d). Following the fornix, fibres only scarcely innervated the posterior and ventral group of nuclei. It is also important to note that a number of fibres were found in the contralateral LS, innervating the same areas as on the ipsilateral side (Figure 6d–f). This bilateral innervation of LS is

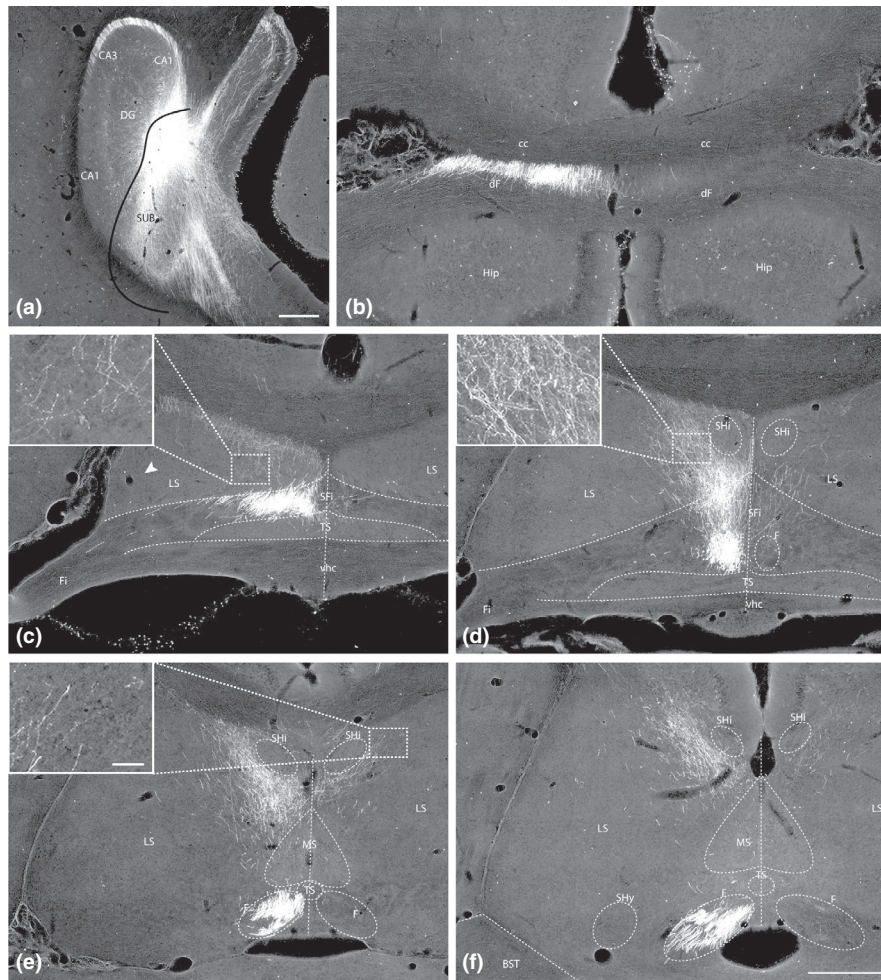


**FIGURE 6** Labelling in the septum resulting from an injection into the dorsal subiculum of a P15 rat. (a), injection site. Scale bar: 500  $\mu$ m. (b–f), Horizontal sections through the septum with 600  $\mu$ m dorsoventral spacing between each two levels depicted from dorsal (b) to ventral (f). (b), Labelled fibres in the dorsal fimbria (dF) just below corpus callosum (cc), reaching the septum at dorsal levels. (c), In the dorsal part of the septum, the labelled fibres are still in the septo-fimbrial nucleus (SFi), approaching the midline. Only a few fibres enter the LS, and they are found medially (magnification box). (d), Section taken at intermediate dorsoventral level of LS revealing more fibres entering the LS. Within LS, fibres originating from dorsal subiculum, with and without varicosities as well as terminating collaterals, travel rostrally and ventrolaterally. (e), Section taken at the dorsal part of medial septal nucleus (MS). Fibres in LS continue their rostral direction close to the midline. Interestingly, most fibres pass around the septo-hippocampal nucleus (SHi), while a few fibres can be seen in the respective field of the contralateral hemisphere (boxed area). Many fibres continue their course in the fornix (F). (f), More ventrally, the terminal field occupies the rostral–medial part of LS. At this level, few labelled fibres can be seen in MS, and no fibres are seen in bed nucleus of stria terminalis (BST). Scale bar in f equals 500  $\mu$ m (valid for a–f). Scale bar in the higher magnification square in e equals 50  $\mu$ m (valid for the magnification boxes in c–e)

unique for the dorsal subiculum as neither intermediate nor ventral subicular injections displayed significant and consistent bilateral septal innervation.

An additional case, with the injection mainly involving the distal dorsal subiculum, with some involvement of the intermediate subiculum and the dentate gyrus, displayed a similar innervation pattern in LS, but the labelling was far weaker. Many labelled fibres travelled through the fimbria reaching the midline of LS, but varicosities or terminating collaterals in the septo-fimbrial nucleus and the triangular septal nucleus were very rarely seen. Few fibres entered LS at the level described above for intermediate subicular injections, and they continued along a comparable course rostro-ventrally and

then laterally. Most of the labelled fibres left the septum by way of the postcommissural fornix, without innervating the posterior and ventral septal nuclei.

Injections involving the border between CA1 and subiculum at dorsal levels, involving neurons from both areas, displayed an innervation pattern of LS very similar to what was seen following the intermediate dorsoventral border injections. Fibres started entering LS upon reaching its dorsolateral edge and more fibres entered LS at a medial medio-lateral level and intermediate dorsoventral level of LS, thus showing the same distribution as the fibres originating from the dorsal subiculum. Furthermore, like intermediate border CA1-subiculum injections, dorsal border injections

displayed relatively strong innervation of the bed nuclei of the anterior commissure and of the stria terminalis.

### 3.4.2 | Ventral subicular projections

Ten injections were successfully aimed at the ventral subiculum of young animals ( $n = 10$ , P6-P17). Labelled fibres could be followed (Figure 7) in the ventrolateral compartment of the fimbria, reaching the septum at its caudo-lateral edge (Figure 7a). The fibres started entering LS ventrally at a lateral medio-lateral level (Figure 7b). In LS, fibres travelled rostrally, occupying the ventral part of LS and extending many thin terminating collaterals (Figure 7c-f). Few passing fibres were labelled, which were directed to the rostral tip of LS and towards the nucleus accumbens (Figure 7e). After leaving LS, labelled fibres curved posteroventrally and joined the fornix, occupying its medial part and the adjacent medial corticohypothalamic tract.

### 3.4.3 | Dorsoventral organization of subicular projections to lateral septum

In order to visualize and better understand the dorsoventral topographic organization of subicular projections to LS, we mapped the injection sites and fibre distributions of three representative injections at dorsal, intermediate and ventral levels onto a series of standard horizontal sections (Figure 8). Fibres from subicular neurons situated at the dorsal part of the hippocampal formation innervated the dorsomedial part of the lateral septal nucleus, and they also had a number of collaterals in the same area of the contralateral hemisphere. Subicular fibres from progressively more ventral levels of the hippocampal formation innervated progressively more lateral and ventral parts of the lateral septal nucleus, without significantly innervating the contralateral hemisphere (Figure 8e-g). In the fimbria, fibres from dorsal subiculum were located dorsally, below the corpus callosum, occupying the medial compartment of fimbria/fornix while passing through the septum. Subicular fibres from progressively more ventral levels of the hippocampal formation were located more ventrally in the fimbria and on their way through the septum they occupied more lateral compartments of the fimbria/fornix (Figure 8d).

In an attempt to even better visualize the complex topological organization of the subicular projections to LS, we produced a 3-dimensional model of the injection site and the fibre trajectories and terminal distribution from the same three representative cases shown in Figure 8. For this purpose, we used the Waxholm Space Atlas of the Sprague Dawley Rat Brain (Figure 9). Projections of the dorsal subiculum are seen to curve around the dorsal end of the hippocampal formation and reach the dorso-caudal side of the

septum through the dorsal fornix. Projections of the intermediate subiculum curve around the lateral side of the hippocampal formation in the alveus and enter the fimbria–fornix occupying a lateral position. Projections from the ventral subiculum also curve around the hippocampal formation in the alveus and then change course towards a more dorsal position until they meet the fimbria. In the fimbria and pre-commissural fornix, those fibres occupy a very ventrolateral position. Moving into the postcommissural fornix, subicular fibres have a different topography. Fibres from intermediate dorsoventral levels of the subiculum are found in the lateral part of the postcommissural fornix, fibres from the dorsal subiculum occupy the intermediate part, whereas fibres from the ventral subiculum curve around the other two subicular fibre bundles from dorsal and intermediate subiculum. While some fibres continue in the medial part of the postcommissural fornix, others continue towards the hypothalamus joining the adjacent medial corticohypothalamic tract.

### 3.5 | The time course of postnatal development of subicular projections to lateral septum

In order to examine the early development and organization of subicular projections into LS, we analysed injections of anterograde tracers in the subiculum of pups aged P01 to P05 ( $n = 7$ ). In all cases, the distribution of the subicular projections was topographically in line with the site of the injection, when compared with comparable injection sites in older animals (Figure 10). However, the total amount of fibres observed in the septum was significantly reduced in these young animals. Fibres were very thin, displaying many varicosities throughout their course but rarely collaterals.

Finally, we examined the postnatal development and organization of subicular projections to LS in older animals, using injections of anterograde tracers in the subiculum of animals aged P18 to P30 ( $n = 10$ ). When comparing intermediate dorsoventral injections in the proximal subiculum at three ages (P7, Figure 11a, b; P14, Figure 11c, d; P24 Figure 11e, f), it is apparent that the labelling patterns in LS are similar, thus showing that the topographic organization of the subicular projections was not altered. However, though with a gradual increase in density over time, our anatomical observations seem to point to a gradual increase density of innervation during postnatal development (Figure 11a, b, compared with c, d, compared with e, f).

## 4 | DISCUSSION

The present study demonstrates, already during postnatal development, a clear topographical organization of the subicular

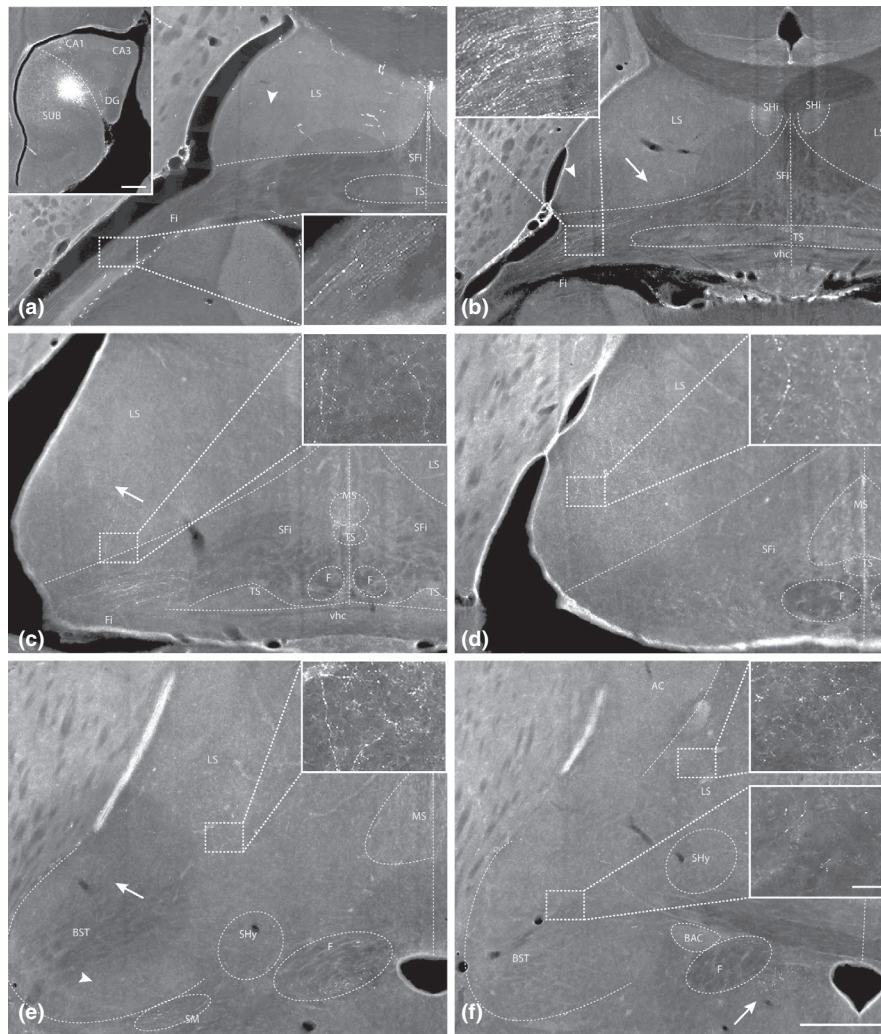


**FIGURE 7** Labelling in the septum resulting from an injection into the ventral subiculum of a P15 rat. Inset in (a), injection site. Scale bar: 500  $\mu\text{m}$ . (a–f), Horizontal sections through the septum with 600  $\mu\text{m}$  dorsoventral spacing between each two levels depicted from dorsal (a) to ventral (f). (a), At a dorsal level, labelled fibres are present in the fimbria (Fi) (magnification box) and no labelled fibres can be seen in septal area (arrowhead). (b), Labelled fibres in fimbria (Fi) reaching septum laterally. At this level, isolated fibres start entering in the LS (arrow) sparing the lateral part of it (arrowhead). (c), Section at ventral levels of the LS revealing more fibres entering LS laterally (boxed area and arrow). (d), Within LS, labelled fibres originating from ventral subiculum branch into a dense plexus of thin terminating collaterals (boxed area). (e, f), At more ventral levels, terminating collaterals occupy the lateral part of LS (boxed areas in e and f) and the septo-hypothalamic nucleus (SHy). Significant innervation can also be seen in the bed nucleus of the stria terminalis (BST) (arrow in e and boxed area in f) where terminating fibres occupy mainly its rostral part and not the caudal one (arrowhead in e). At this ventral level, a number of labelled fibres from ventral subiculum curve around postcommissural fornix and few of them continue in the medial part of the postcommissural fornix and most of them in the adjacent medial corticohypothalamic tract (arrow in f). Scale bar in f equals 500  $\mu\text{m}$  (valid for a–f). Scale bar in the higher magnification square in f equals 50  $\mu\text{m}$  (valid for the magnification boxes in a–f)

projections to LS depending on the dorsoventral level of origin in the subiculum. Our findings are in accordance with the topographical organization previously described in the adult brain (Meibach & Siegel, 1977a). Fibres from subicular neurons situated at the dorsal part of the hippocampal formation innervate the dorsomedial part of LS, whereas subicular fibres from progressively more ventral levels innervate progressively more lateral and ventral parts of LS. This topographic organization is present at the first postnatal days, and it is preserved throughout the postnatal development of the rat brain.

We provide additional data demonstrating that changes in the origin along the transverse axis of the subiculum do not change the topographic pattern of septal innervation significantly but correspond to changing density and branching complexity of the subicular axons. Projections originating in the proximal part of the subiculum provide a dense innervation of LS and progressively more distal parts send an increasingly sparser projection to LS.

The 3-dimensional model allowed us to visualize the topographical complexity of the fibre trajectories in planes

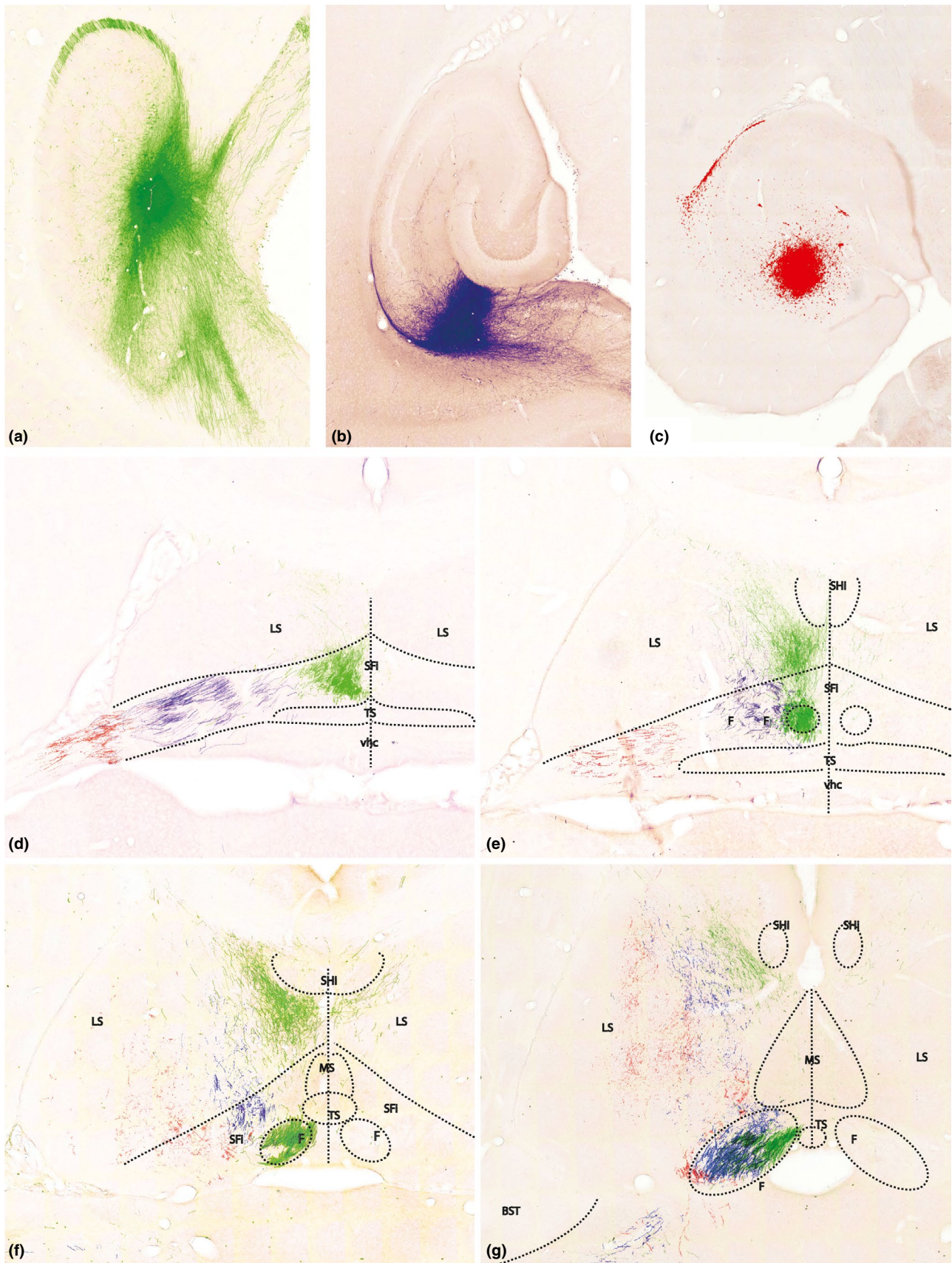


**FIGURE 8** Comparative distribution of subicular projections into LS after dorsal (a, green), intermediate (b, blue) and ventral (c, red) injections. For illustrative purposes, three separate cases were false-coloured and overlaid on top of one another. Horizontal sections through septum are displayed from dorsal to ventral (d–g) [Colour figure can be viewed at [wileyonlinelibrary.com](http://wileyonlinelibrary.com)]

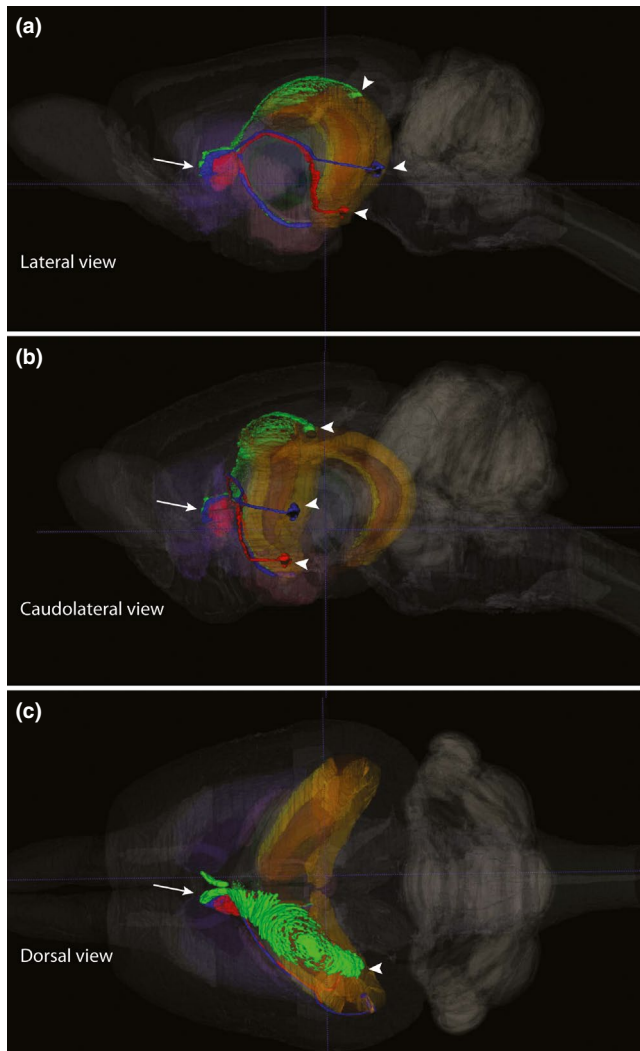


**FIGURE 9** Three-dimensional model of the injection site and the fibre course from the same three cases presented in Figure 8, using the Waxholm Space Atlas of the Sprague Dawley Rat Brain. The three different injection sites are labelled with arrowheads and the distribution of fibres into LS with arrows [Colour figure can be viewed at [wileyonlinelibrary.com](http://wileyonlinelibrary.com)]

different from those that we initially used. With the use of this model approach, we could examine the topography of the subicular fibres in the coronal plane in order to compare the observed terminal distribution with the subdivisions of LS as previously described (Risold & Swanson, 1997). We found that subicular fibres in LS only partly respect this compartmentalization. Fibres from the dorsal subiculum occupy the dorsal region of the rostral part of LS, and fibres from ventral subiculum occupy the ventral region of the rostral part of LS and the ventral part of the LS (Risold & Swanson, 1997).

The hippocampal formation displays a significant heterogeneity regarding the main input and output connections and the kind of information processed along its longitudinal axis (Cappaert, 2015; Moser & Moser, 1998; Naber & Witter, 1998; Strange, Witter, Lein, & Moser,

2014). The dorsal hippocampus is strongly implicated in spatial and non-spatial learning and memory (Cohen et al., 2013; Moser, Moser, & Andersen, 1993), and the ventral hippocampus is implicated in social memory, emotional processing and anxiety (Chen, Wang, Wang, & Li, 2017; Felix-Ortiz & Tye, 2014; Okuyama, 2017). Our data indicate that this dorsoventral organization is reflected in the projections from subiculum to LS and that this topography is already present from the first postnatal days and is stable during postnatal development.

Similar to the well-established topography dictated by the longitudinal or dorsoventral axis, the transverse axis has also been established as a main organizational principle for intrinsic hippocampal circuitry, particularly prominent in the projections from CA3 to CA1 (Ishizuka, Weber, & Amaral, 1990) and even more so for those of CA1 to subiculum (Amaral, Dolorfo, & Alvarez-Royo, 1991). A comparable transverse organization has been reported for the parallel reciprocal connections between subiculum and the lateral and medial entorhinal cortex, where lateral entorhinal cortex preferentially connects with proximal subiculum and medial entorhinal cortex connects with distal subiculum (Witter, Wouterlood, Naber, & Haeflén, 2000). Finally, efferent subicular projections are organized in the same way, such that projections to different brain regions, or different parts of the same brain region, originate from the proximal, middle and distal thirds of the subiculum (Witter et al., 1990). These reports include a preferred proximal origin of LS projections, and as we showed in the present study, this organization is already present from birth.

Our data included injections that were not confined to proximal subiculum, but also involved distal CA1. In those cases, we consistently, and independent of age, observed additional projections to the bed nuclei of the anterior commissure and the stria terminalis, which were not observed in cases of subicular projections. The border area between CA1 and subiculum, by some authors referred to as prosubiculum, innervates the bed nucleus of stria terminalis in adult rats and mice as well (Ding, 2013; Howell, Perez-Clausell, & Frederickson, 1991).

Finally, the present findings demonstrate that the postnatal development of subicular projections to LS preferentially features axonal expansion rather than axonal pruning. Several mechanisms have been proposed for the development of projections in the central nervous system. Both activity-independent and activity-dependent mechanisms regulate the navigation of axons during development (Olavarria & Safaeian, 2006; Price et al., 2006). Further, early embryonic outgrowth of axons is directed mainly by molecular cues (Garel & Rubenstein, 2004). The postnatal axonal development is governed by two different mechanisms, the specific ingrowth and elaboration of axon branches at topographically correct places (Olavarria & Safaeian, 2006)

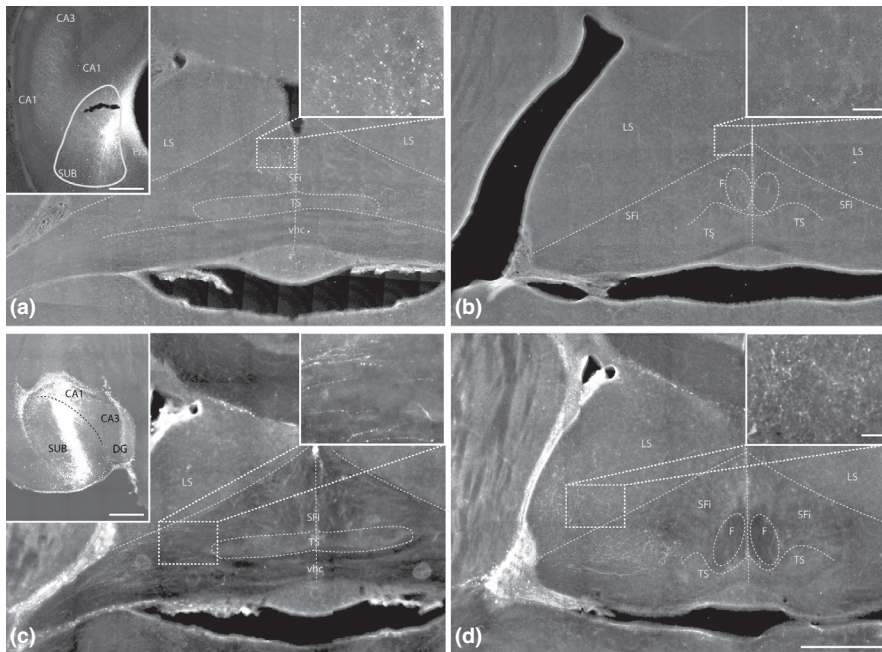


**FIGURE 10** The early development of subicular projections to LS. (a, b), A P3 case with injection of anterograde tracer into dorsal subiculum (inset in a—scale bar: 500  $\mu\text{m}$ ). (c, d), A P3 case with injection into ventral subiculum (inset in c—scale bar: 500  $\mu\text{m}$ ). Note that in both cases, the distribution pattern of fibres is identical to that of older animals, though the fibres of these young animals are thinner, with many varicosities and few collaterals. Scale bar in d equals 500  $\mu\text{m}$  (valid for a–d). Scale bar in the higher magnification squares in b and d equals 50  $\mu\text{m}$  (also valid for the magnification boxes in a and c, respectively)

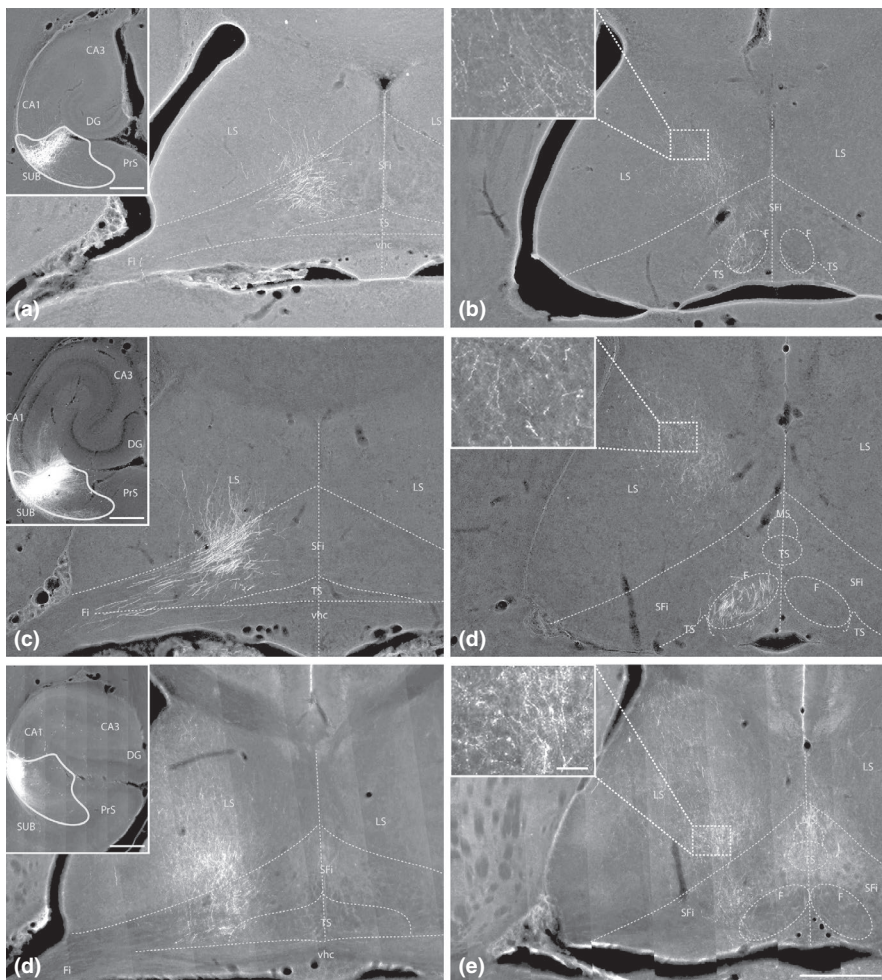


**FIGURE 11** Labelling in the septum resulting from three representative injections at approximately the same intermediate dorsoventral level into the proximal part of the subiculum in P7 (a, b), P14 (c, d) and P24 (e, f) pups. Insets in a, c and e: injection sites. Scale bar: 500  $\mu\text{m}$ . (a, c, e), Horizontal sections taken at the level where labelled fibres in the fimbria (Fi) start entering LS. Note the difference in the density of these fibres from a to e. (b, d, f), Horizontal sections at intermediate dorsoventral level of the LS. An apparent increase in the innervation density of LS seems present from b to f. Scale bar in f equals 500  $\mu\text{m}$  (valid for a–f). Scale bar in the magnification square in f equals 50  $\mu\text{m}$  (valid for the magnification boxes in b, d, f)

or the exuberant development of connections followed by axonal selection and pruning (Innocenti & Price, 2005). These two mechanisms have been alternatively described in

different neuronal networks as well as in different species (Price et al., 2006). We conclude that the development of subicular projections to LS follows the former mechanism

which seems a common finding in the cortical–hippocampal system, as similar observations have been published in case of subicular projections to parahippocampal areas (O'Reilly et al., 2013), for the entorhinal–hippocampal and retrosplenial–entorhinal projections (O'Reilly et al., 2015; Sugar et al., 2011), as well as for pre- and parasubicular projections to the medial entorhinal cortex (Canto et al., 2019).

## ACKNOWLEDGEMENTS

This study was supported through the Centre of Excellence Scheme and the National Infrastructure Scheme of the Research Council of Norway (Centre for Neural Computation, grant number 223262; NORBRAIN1, grant number 197467). The authors thank Bruno Monterotti for assistance with histology. KIT was supported by IBRO-PERC InEurope Short Stay Grant 2014, ENS Fellowship 2014 and Genesis Pharma for his stay in Trondheim.

## CONFLICT OF INTEREST

The authors disclose no conflicts of interest.

## AUTHORS' CONTRIBUTIONS

K.I.T. acquired and analysed the data, prepared all figures and wrote the manuscript. M.J.D.L., A.G.D. and K.C.O'R designed and performed experiments, and acquired data. M.P.W. designed the study and supervised the preparation of the manuscript.

## DATA ACCESSIBILITY

All data are freely available upon request. Please contact the corresponding author. The 3-dimensional model of the course of the axons from subiculum to LS on the Waxholm Space Atlas of the Sprague Dawley Rat Brain is made available online in Figshare.

## ORCID

Menno P. Witter  <https://orcid.org/0000-0003-0285-1637>

## REFERENCES

- Amaral, D. G., Dolorfo, C., & Alvarez-Royo, P. (1991). Organization of CA1 projections to the subiculum: A PHA-L analysis in the rat. *Hippocampus*, *1*, 415–435. <https://doi.org/10.1002/hipo.450010410>
- Amaral, D. G., & Kurz, J. (1985). An analysis of the origins of the cholinergic and noncholinergic septal projections to the hippocampal formation of the rat. *The Journal of Comparative Neurology*, *240*, 37–59. <https://doi.org/10.1002/cne.902400104>
- Baisden, R. H., Woodruff, M. L., & Hoover, D. B. (1984). Cholinergic and non-cholinergic septo-hippocampal projections: A double-label horseradish peroxidase-acetylcholinesterase study in the rabbit. *Brain Research*, *290*, 146–151. [https://doi.org/10.1016/0006-8993\(84\)90745-5](https://doi.org/10.1016/0006-8993(84)90745-5)
- Bender, F., Gorbati, M., Cadavieco, M. C., Denisova, N., Gao, X., Holman, C., ... Ponomarenko, A. (2015). Theta oscillations regulate the speed of locomotion via a hippocampus to lateral septum

- pathway. *Nature Communications*, *6*, 8521. <https://doi.org/10.1038/ncomms9521>
- Calfa, G., Bussolino, D., & Molina, V. A. (2007). Involvement of the lateral septum and the ventral Hippocampus in the emotional sequelae induced by social defeat: Role of glucocorticoid receptors. *Behavioural Brain Research*, *181*, 23–34. <https://doi.org/10.1016/j.bbr.2007.03.020>
- Canto, C. B., Koganezawa, N., Lagartos-Donate, M. J., O'Reilly, K. C., Mansvelter, H. D., & Witter, M. P. (2019). Postnatal development of functional projections from parasubiculum and presubiculum to medial entorhinal cortex in the rat. *Journal of Neuroscience*, *39*, 8645–8663. <https://doi.org/10.1523/JNEUROSCI.1623-19.2019>
- Cappaert, N. L. M., Van Strien, N. M., & Witter, M. P. (2015). Hippocampal formation. In G. Paxinos (Eds.), *The rat nervous system* (pp. 511–560). Oxford, UK: Elsevier.
- Chen, W., Wang, Y., Wang, X., & Li, H. (2017). Neural circuits involved in the renewal of extinguished fear. *IUBMB Life*, *69*, 470–478. <https://doi.org/10.1002/iub.1636>
- Cohen, S. J., Munchow, A. H., Rios, L. M., Zhang, G., Asgeirsdottir, H. N., & Stackman, R. W. Jr (2013). The rodent hippocampus is essential for nonspatial object memory. *Current Biology*, *23*, 1685–1690. <https://doi.org/10.1016/j.cub.2013.07.002>
- Colom, L. V. (2006). Septal networks: Relevance to theta rhythm, epilepsy and Alzheimer's disease. *Journal of Neurochemistry*, *96*, 609–623. <https://doi.org/10.1111/j.1471-4159.2005.03630.x>
- Ding, S. L. (2013). Comparative anatomy of the prosubiculum, subiculum, presubiculum, postsubiculum, and parasubiculum in human, monkey, and rodent. *The Journal of Comparative Neurology*, *521*, 4145–4162. <https://doi.org/10.1002/cne.23416>
- Easton, A., Douchamps, V., Eacott, M., & Lever, C. (2012). A specific role for septohippocampal acetylcholine in memory? *Neuropsychologia*, *50*, 3156–3168. <https://doi.org/10.1016/j.neuropsychologia.2012.07.022>
- Felix-Ortiz, A. C., & Tye, K. M. (2014). Amygdala inputs to the ventral hippocampus bidirectionally modulate social behavior. *Journal of Neuroscience*, *34*, 586–595. <https://doi.org/10.1523/JNEUROSCI.4257-13.2014>
- Garel, S., & Rubenstein, J. L. (2004). Intermediate targets in formation of topographic projections: Inputs from the thalamocortical system. *Trends in Neurosciences*, *27*, 533–539. <https://doi.org/10.1016/j.tins.2004.06.014>
- Gaykema, R. P., Luiten, P. G., Nyakas, C., & Traber, J. (1990). Cortical projection patterns of the medial septum-diagonal band complex. *The Journal of Comparative Neurology*, *293*, 103–124. <https://doi.org/10.1002/cne.902930109>
- Gaykema, R. P., van der Kuil, J., Hersh, L. B., & Luiten, P. G. (1991). Patterns of direct projections from the hippocampus to the medial septum-diagonal band complex: Anterograde tracing with *Phaseolus vulgaris* leucoagglutinin combined with immunohistochemistry of choline acetyltransferase. *Neuroscience*, *43*, 349–360. [https://doi.org/10.1016/0306-4522\(91\)90299-4](https://doi.org/10.1016/0306-4522(91)90299-4)
- Haugland, K. G., Sugar, J., & Witter, M. P. (2019). Development and topographical organization of projections from the hippocampus and parahippocampus to the retrosplenial cortex. *European Journal of Neuroscience*, *50*, 1799–1819. <https://doi.org/10.1111/ejn.14395>
- Howell, G. A., Perez-Clausell, J., & Frederickson, C. J. (1991). Zinc containing projections to the bed nucleus of the stria terminalis. *Brain Research*, *562*, 181–189. [https://doi.org/10.1016/0006-8993\(91\)90620-B](https://doi.org/10.1016/0006-8993(91)90620-B)

- Hunsaker, M. R., Rogers, J. L., & Kesner, R. P. (2007). Behavioral characterization of a transection of dorsal CA3 subcortical efferents: Comparison with scopolamine and physostigmine infusions into dorsal CA3. *Neurobiology of Learning and Memory*, *88*, 127–136. <https://doi.org/10.1016/j.nlm.2007.01.006>
- Hunsaker, M. R., Tran, G. T., & Kesner, R. P. (2009). A behavioral analysis of the role of CA3 and CA1 subcortical efferents during classical fear conditioning. *Behavioral Neuroscience*, *123*, 624–630. <https://doi.org/10.1037/a0015455>
- Innocenti, G. M., & Price, D. J. (2005). Exuberance in the development of cortical networks. *Nature Reviews Neuroscience*, *6*, 955–965. <https://doi.org/10.1038/nrn1790>
- Ishizuka, N., Weber, J., & Amaral, D. G. (1990). Organization of intra-hippocampal projections originating from CA3 pyramidal cells in the rat. *The Journal of Comparative Neurology*, *295*, 580–623. <https://doi.org/10.1002/cne.902950407>
- Jonsson, S., Morud, J., Stomberg, R., Ericson, M., & Soderpalm, B. (2017). Involvement of lateral septum in alcohol's dopamine-elevating effect in the rat. *Addiction Biology*, *22*, 93–102. <https://doi.org/10.1111/adb.12297>
- Kitchigina, V., Popova, I., Sinelnikova, V., Malkov, A., Astasheva, E., Shubina, L., & Aliev, R. (2013). Disturbances of septohippocampal theta oscillations in the epileptic brain: Reasons and consequences. *Experimental Neurology*, *247*, 314–327. <https://doi.org/10.1016/j.expneurol.2013.01.029>
- Linke, R., Pabst, T., & Frotscher, M. (1995). Development of the hippocamposeptal projection in the rat. *The Journal of Comparative Neurology*, *351*, 602–616. <https://doi.org/10.1002/cne.903510409>
- McGlinchey, E. M., & Aston-Jones, G. (2017). Dorsal hippocampus drives context-induced cocaine seeking via inputs to lateral septum. *Neuropsychopharmacology*, *43*(5), 987–1000. <https://doi.org/10.1038/npp.2017.144>
- Meibach, R. C., & Siegel, A. (1977a). Efferent connections of the hippocampal formation in the rat. *Brain Research*, *124*, 197–224. [https://doi.org/10.1016/0006-8993\(77\)90880-0](https://doi.org/10.1016/0006-8993(77)90880-0)
- Meibach, R. C., & Siegel, A. (1977b). Efferent connections of the septal area in the rat: An analysis utilizing retrograde and anterograde transport methods. *Brain Research*, *119*, 1–20. [https://doi.org/10.1016/0006-8993\(77\)90088-9](https://doi.org/10.1016/0006-8993(77)90088-9)
- Moser, E., Moser, M. B., & Andersen, P. (1993). Spatial learning impairment parallels the magnitude of dorsal hippocampal lesions, but is hardly present following ventral lesions. *Journal of Neuroscience*, *13*, 3916–3925. <https://doi.org/10.1523/JNEUROSCI.13-09-03916.1993>
- Moser, M. B., & Moser, E. I. (1998). Functional differentiation in the hippocampus. *Hippocampus*, *8*, 608–619. [https://doi.org/10.1002/\(SICI\)1098-1063\(1998\)8:6<608:AID-HIPO3>3.0.CO;2-7](https://doi.org/10.1002/(SICI)1098-1063(1998)8:6<608:AID-HIPO3>3.0.CO;2-7)
- Naber, P. A., & Witter, M. P. (1998). Subicular efferents are organized mostly as parallel projections: A double-labeling, retrograde-tracing study in the rat. *The Journal of Comparative Neurology*, *393*, 284–297. [https://doi.org/10.1002/\(SICI\)1096-9861\(19980413\)393:3<284:AID-CNE2>3.0.CO;2-Y](https://doi.org/10.1002/(SICI)1096-9861(19980413)393:3<284:AID-CNE2>3.0.CO;2-Y)
- Nyakas, C., Luiten, P. G., Spencer, D. G., & Traber, J. (1987). Detailed projection patterns of septal and diagonal band efferents to the hippocampus in the rat with emphasis on innervation of CA1 and dentate gyrus. *Brain Research Bulletin*, *18*, 533–545. [https://doi.org/10.1016/0361-9230\(87\)90117-1](https://doi.org/10.1016/0361-9230(87)90117-1)
- Okada, K., & Okaichi, H. (2010). Functional cooperation between the hippocampal subregions and the medial septum in unreinforced and reinforced spatial memory tasks. *Behavioural Brain Research*, *209*, 295–304. <https://doi.org/10.1016/j.bbr.2010.02.007>
- Okuyama, T. (2017). Social memory engram in the hippocampus. *Neuroscience Research*, *129*, 17–23. <https://doi.org/10.1016/j.neures.2017.05.007>
- Olavarria, J. F., & Safaeian, P. (2006). Development of callosal topography in visual cortex of normal and enucleated rats. *The Journal of Comparative Neurology*, *496*, 495–512. <https://doi.org/10.1002/cne.20938>
- O'Reilly, K. C., Flatberg, A., Islam, S., Olsen, L. C., Kruge, I. U., & Witter, M. P. (2015). Identification of dorsal-ventral hippocampal differentiation in neonatal rats. *Brain Structure and Function*, *220*, 2873–2893. <https://doi.org/10.1007/s00429-014-0831-8>
- O'Reilly, K. C., Gulden Dahl, A., Ulsaker Kruge, I., & Witter, M. P. (2013). Subicular-parahippocampal projections revisited: Development of a complex topography in the rat. *The Journal of Comparative Neurology*, *521*, 4284–4299. <https://doi.org/10.1002/cne.23417>
- Parent, M. B., & Baxter, M. G. (2004). Septohippocampal acetylcholine: Involved in but not necessary for learning and memory? *Learning & Memory*, *11*, 9–20. <https://doi.org/10.1101/lm.69104>
- Price, D. J., Kennedy, H., Dehay, C., Zhou, L., Mercier, M., Jossin, Y., ... Molnar, Z. (2006). The development of cortical connections. *European Journal of Neuroscience*, *23*, 910–920. <https://doi.org/10.1111/j.1460-9568.2006.04620.x>
- Risold, P. Y., & Swanson, L. W. (1997). Chemoarchitecture of the rat lateral septal nucleus. *Brain Research. Brain Research Reviews*, *24*, 91–113.
- Singh, S. C. (1977). The development of olfactory and hippocampal pathways in the brain of the rat. *Anatomy and Embryology*, *151*, 183–199. <https://doi.org/10.1007/BF00297480>
- Strange, B. A., Witter, M. P., Lein, E. S., & Moser, E. I. (2014). Functional organization of the hippocampal longitudinal axis. *Nature Reviews Neuroscience*, *15*, 655–669. <https://doi.org/10.1038/nrn3785>
- Sugar, J., Witter, M. P., van Strien, N. M., & Cappaert, N. L. (2011). The retrosplenial cortex: Intrinsic connectivity and connections with the (para)hippocampal region in the rat. An Interactive Connectome. *Frontiers in Neuroinformatics*, *5*, 7. <https://doi.org/10.3389/fninf.2011.00007>
- Super, H., & Soriano, E. (1994). The organization of the embryonic and early postnatal murine hippocampus. II. Development of entorhinal, commissural, and septal connections studied with the lipophilic tracer DiI. *The Journal of Comparative Neurology*, *344*, 101–120.
- Swanson, L. W., & Cowan, W. M. (1977). An autoradiographic study of the organization of the efferent connections of the hippocampal formation in the rat. *The Journal of Comparative Neurology*, *172*, 49–84.
- Swanson, L. W., & Cowan, W. M. (1979). The connections of the septal region in the rat. *The Journal of Comparative Neurology*, *186*, 621–655. <https://doi.org/10.1002/cne.901860408>
- Tsanov, M. (2015). Septo-hippocampal signal processing: Breaking the code. *Progress in Brain Research*, *219*, 103–120.
- Unal, G., Joshi, A., Viney, T. J., Kis, V., & Somogyi, P. (2015). Synaptic targets of medial septal projections in the hippocampus and extrahippocampal cortices of the mouse. *Journal of Neuroscience*, *35*(48), 15812–15826. <https://doi.org/10.1523/JNEUROSCI.2639-15.2015>
- Witter, M. P., & Groenewegen, H. J. (1986). Connections of the parahippocampal cortex in the cat. IV. Subcortical efferents. *The Journal of Comparative Neurology*, *252*, 51–77. <https://doi.org/10.1002/cne.902520104>
- Witter, M. P., Ostendorf, R. H., & Groenewegen, H. J. (1990). Heterogeneity in the dorsal subiculum of the rat. Distinct

- neuronal zones project to different cortical and subcortical targets. *The European Journal of Neuroscience*, 2, 718–725. <https://doi.org/10.1111/j.1460-9568.1990.tb00462.x>
- Witter, M. P., Wouterlood, F. G., Naber, P. A., & Van Haeften, T. (2000). Anatomical organization of the parahippocampal-hippocampal network. *Annals New York Academy of Science*, 911, 1–24. <https://doi.org/10.1111/j.1749-6632.2000.tb06716.x>
- Zhou, T. L., Tamura, R., Kuriwaki, J., & Ono, T. (1999). Comparison of medial and lateral septal neuron activity during performance of spatial tasks in rats. *Hippocampus*, 9, 220–234. [https://doi.org/10.1002/\(SICI\)1098-1063\(1999\)9:3<220:AID-HIPO3>3.0.CO;2-E](https://doi.org/10.1002/(SICI)1098-1063(1999)9:3<220:AID-HIPO3>3.0.CO;2-E)
- Zoicas, I., Slattery, D. A., & Neumann, I. D. (2014). Brain oxytocin in social fear conditioning and its extinction: Involvement of the lateral

septum. *Neuropsychopharmacology*, 39, 3027–3035. <https://doi.org/10.1038/npp.2014.156>

**How to cite this article:** Tsamis KI, Lagartos Donato MJ, Dahl AG, O'Reilly KC, Witter MP. Development and topographic organization of subicular projections to lateral septum in the rat brain. *Eur J Neurosci*. 2020;52:3140–3159. <https://doi.org/10.1111/ejn.14696>